Letter

Quantum criticality linked to the suppressed superconducting upper critical field in Ni-doped CeCoIn₅

Azumi Yashiro, ^{1,2} Rahmanto, ^{1,2} Kaketo Inami, ³ Kohei Suzuki, ^{1,2} Kaede Inoh, ^{1,2} Teppei Takahashi, ^{1,2} Ryosuke Koizumi, ^{1,2} Yohei Kono, ³ Shunichiro Kittaka, ³ Yusei Shimizu, ⁴ Fuminori Honda, ^{4,*} Dai Aoki, ⁴ Kenichi Tenya, ⁵ and Makoto Yokoyama ^{1,2,†}

¹ Faculty of Science, Ibaraki University, Mito, Ibaraki 310-8512, Japan
² Institute of Quantum Beam Science, Ibaraki University, Mito, Ibaraki 310-8512, Japan
³ Department of Physics, Chuo University, Bunkyo-ku, Tokyo 112-8551, Japan
⁴ Institute for Materials Research, Tohoku University, Oarai, Ibaraki 311-1313, Japan
⁵ Faculty of Education, Shinshu University, Nagano 380-8544, Japan

(Received 8 February 2024; accepted 17 July 2024; published 8 August 2024)

We demonstrate a close connection between the quantum critical point (QCP) and superconducting upper critical field H_{c2} in the Ni-doped heavy-fermion superconductor CeCoIn₅. Temperature variations of electrical resistivity $\rho(T)$ exhibit a crossover between the non-Fermi liquid and the Fermi liquid states, whose boundary for $T \to 0$, regarded as the QCP, coincides with H_{c2} , while H_{c2} decreases to zero with increasing Ni concentrations up to 25%. Furthermore, the A coefficient of the T^2 term in $\rho(T)$ estimated in the Fermi liquid region shows the diverging behavior with decreasing the magnetic field H toward H_{c2} . These experimental results suggest that the emergence of the QCP is always accompanied by the breakdown of the superconducting state by H in Ni-doped CeCoIn₅.

DOI: 10.1103/PhysRevMaterials.8.L081801

Understanding the interplay of quantum criticality and unconventional superconductivity has been challenging in strongly correlated electron systems [1-3]. The heavyfermion compound CeCoIn₅ [the HoCoGa₅-type tetragonal structure, see Fig. 3(b)] is one of the most investigated superconductors from such a perspective [4]. It exhibits a superconducting (SC) order below $T_c = 2.3$ K characterized by an anomalously large specific heat jump of $\Delta C/\gamma T_c = 4.5$ [4], and its order parameter involves a d-wave gap symmetry [5–7]. In a magnetic field H, a strong Pauli paramagnetic effect yields a first-order transition at the SC upper critical field H_{c2} , and the other SC state coexisting with incommensurate antiferromagnetic (AFM) states, termed the Q phase, emerges just below H_{c2} for H along the tetragonal c plane [5,8–17]. It is expected that the AFM spin correlations underlie all of the unusual features above concerning the SC state in CeCoIn₅.

The AFM correlation effects manifest themselves in the paramagnetic region above $\mu_0 H_{c2} = 5$ T (μ_0 : vacuum permeability) for $H \mid\mid c$, such as a $-\ln T$ divergence in specific heat divided by temperature C/T, T-linear behavior in electrical resistivity, and a strong enhancement of the nuclear spin-lattice relaxation rate [18–22]. These non-Fermi liquid (NFL) behaviors are attributed to the quantum criticality originating from hidden AFM order parameters [18–20] because the AFM orders continuously evolve with doping Rh (a congener) [23–27], Cd [28–31], Hg [28,32], Zn [33–39] (possible hole dopants), Nd [40–42], and Sm [43] (magnetic ions) into

CeCoIn₅. Moreover, possible field-induced AFM ordering at extremely low temperatures ($T \sim 20 \text{ mK}$) is proposed for pure CeCoIn₅ [44,45].

In contrast to the doping effects above, a paramagnetic state becomes stable due to the suppression of the SC order when the In and Co ions are substituted by Sn [46–48] and Ni [49–51], respectively, which are expected to act as the electron dopants in CeCoIn₅. Recent investigations for CeCo_{1-x}Ni_xIn₅ have revealed that the SC transition temperature T_c and H_{c2} along the c axis continuously decrease toward zero as x is increased up to the critical Ni concentration: $x_c = 0.25$ [49]. In addition, the NFL behaviors occur in the paramagnetic phase at x_c , characterized by $-\ln T$ diverging behavior in C/T, a $T^{-\eta}$ ($\eta \sim 0.2$) increase in magnetization M/H, a nearly Tlinear dependence in electrical resistivity ρ , and a significant reduction in the nuclear spin-lattice relaxation rate for $T \to 0$ at $H \sim 0$ [49–51]. These features strongly suggest that the AFM quantum criticality survives through the shrinkage of the SC order. Accordingly, the tetragonal structure does not change with the doping of Ni ions. The effective magnetic moment for $x \le 0.3$ is nearly independent of x and coincides well with that calculated from the J = 5/2 multiplet in the Ce³⁺ ion [49], suggesting that the Ce 4f electrons are responsible for the magnetic properties in pure and Ni-doped CeCoIn₅.

Presently, it is unclear how the quantum criticality of 25% Ni-doped CeCoIn₅ is connected with that of the pure compound and the AFM orders induced in other doped alloys. Thus far, two types of AFM phases were found in Zn-doped CeCoIn₅, corresponding to the commensurate and incommensurate AFM phases, and their quantum critical points (QCPs) are located at zero and finite magnetic fields, respectively [36–38]. In this regard, it is interesting to investigate which

^{*}Present address: Central Institute of Radioisotope Science and Safety Management, Kyushu University, Fukuoka 819-0395, Japan. †Contact author: makoto.yokoyama.sci@vc.ibaraki.ac.jp

QCP is linked with the quantum critical behavior emerging in 25% Ni-doped CeCoIn₅. Electrical resistivity is a useful probe for investigating quantum criticality because it can frequently be captured as a deviation from the T^2 dependence expected from the Fermi liquid (FL) theory and a diverging feature in a coefficient of the T^2 function toward the QCP [20,52–55]. Thus, we investigated the connection between the QCPs of pure and 25% Ni-doped CeCoIn₅ using the electrical resistivity measurements.

Single crystals of $CeCo_{1-x}Ni_xIn_5$ for $x \le 0.25$ were grown via an indium-flux method, details of which are described elsewhere [49]. Note that the inductively coupled plasma mass spectrometry measurements indicate that the actual Ni concentration approximately coincides with the starting (nominal) value within the deviation of $\Delta x/x \sim 17\%$, including the experimental error [49]. Hereafter, the nominal x values are used for simplicity. Square bars with a typical dimension of $\sim 3 \text{ mm} \times 0.9 \text{ mm}^2$ were cut out from the plate-shaped crystals. Electrical resistivity ρ was measured using a commercial measurement system (PPMS, Quantum Design) ($T \ge$ 0.3 K) and an ac four-probe method in a dilution refrigerator (Kelvinox AST Minisorb, Oxford) $(0.1 \le T \le 1.5 \text{ K})$. The magnetic field $\mu_0 H$ was applied at up to 9 T along the c axis, perpendicular to the direction of a current j ($\parallel a$). We confirmed that a Hall component in the ρ data caused by wiring conditions was negligible. The residual resistivity ratio, defined as $\rho(300 \text{ K})/\rho(2.5 \text{ K})$, was 3.01(1) (x = 0.125), 3.11(1)(x = 0.2), and 3.56(1) (x = 0.25), which are comparable to those in the previous measurements [49]. We also checked that the T_c and H_{c2} values estimated in the present resistivity measurements are consistent with those obtained from the previous samples [49], as plotted in Fig. 2.

Figure 1 shows the low-temperature electrical resistivity for (a) x = 0.125, (b) 0.2, and (c) 0.25, plotted as a function of T^2 . These insets display the overall behaviors in the temperature variations of resistivity $\rho(T)$ below room temperature for H = 0. At zero field, the $\rho(T)$ curves for x = 0.125, 0.2, and 0.25 involve zero resistivity due to the SC order [the inset in Figs. 1(a)–1(c)], and the transition temperatures for x = 0.125and 0.2 are consistent with those reported previously [49]. However, in the x = 0.25 sample, the two-step drops unexpectedly occur in ρ below ~ 0.4 K for H=0, although the specific heat measurement down to 0.3 K and the nuclearquadrupole-resonance (NQR) and ac-magnetic-susceptibility measurements down to 0.1 K do not indicate the SC transition even at H = 0 [50,51]. It is considered that a small fragment of the SC region caused by a slight distribution of Ni concentration in the sample yields the two-step drops because T_c steeply decreases around $x_c = 0.25$ in the Ni concentration versus temperature (x-T) phase diagram [Fig. 3(a)] [49]. We confirmed that this SC state is suppressed by applying a weak field of less than 1 T.

At low temperatures, the ρ data for low fields just above $\mu_0 H_{c2}(T \to 0)$ [2.6(1) T (x = 0.125), 1.6(1) T (x = 0.2), and ~ 0 (x = 0.25)] involve a convex upward when plotted as a function of T^2 [Figs. 1(a)–1(c)], which is regarded as the NFL behavior characterized by the T^n dependence on ρ with $n \sim 1$ [49]. This feature is suppressed, and a $\rho \propto AT^2$ relation (A: a coefficient) becomes dominant with increasing H, reflecting a crossover from the NFL to FL states with H. We define the

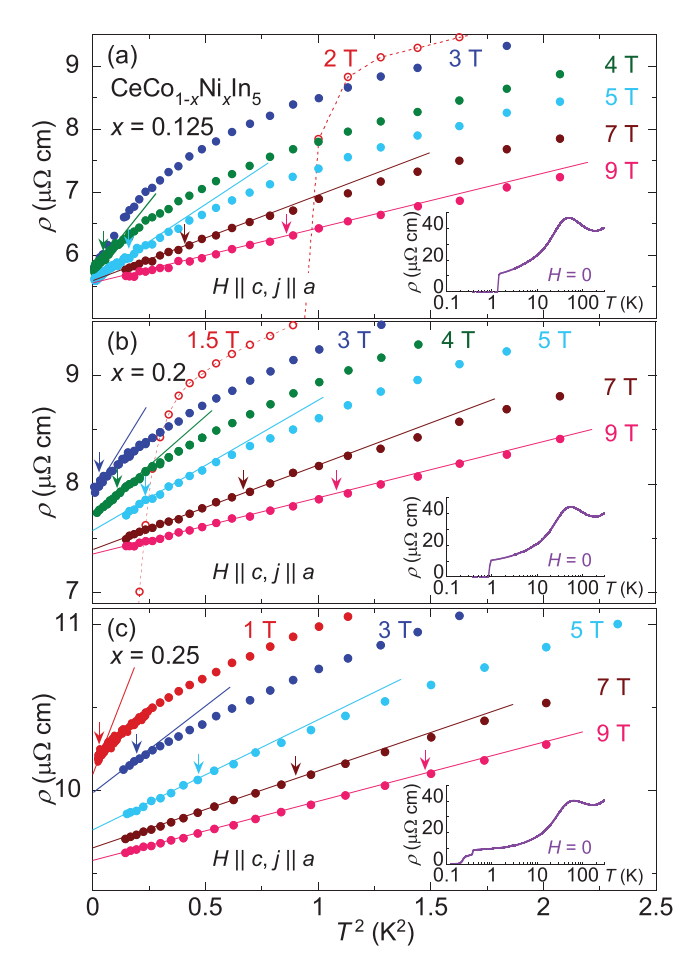


FIG. 1. Low-temperature electrical resistivity ρ plotted as a function of T^2 for $\text{CeCo}_{1-x}\text{Ni}_x\text{In}_5$ with (a) x=0.125, (b) 0.2, and (c) 0.25 obtained under the $H \mid c$ and $j \mid a$ conditions. The solid lines are a guide for the function of $\rho \propto AT^2$, and the arrows indicate the crossover temperature T_{FL} between the FL and NFL states determined by the deviation from the T^2 function. The insets display the temperature variations of ρ for H=0.

NFL–FL crossover temperature $T_{\rm FL}$ by the deviation from the T^2 dependence of ρ [the arrows in Figs. 1(a)–1(c)], mainly estimated using the $d\rho/d(T^2)$ curves [see the Supplemental Material [56] for the details]. $T_{\rm FL}$ is reduced with decreasing H for all the Ni concentrations investigated. Although the NFL behavior becomes pronounced in $\rho(T)$ at low fields, $\rho(T)$ involves the T^2 behavior in a small T region at very low temperatures, similar to those seen in $\rho(T)$ above H_{c2} for CeCoIn₅ [20].

In Fig. 2, we plot the magnetic field versus temperature (H-T) phase diagram for (a) x=0.125, (b) 0.2, and (c) 0.25, obtained from the $T_{\rm FL}$ and H_{c2} values. For the entire x range investigated, $T_{\rm FL}$ is linearly reduced with decreasing H and then approaches $H_{c2}(T=0)$ for $T\to 0$. The near coincidence of the rate $dT_{\rm FL}/\mu_0 dH \sim 0.14$ K/T for $x\leqslant 0.25$ implies that the electronic and spin states responsible for the NFL–FL crossover are roughly unchanged with the Ni doping. Because the QCP is expected to exist at the NFL–FL boundary at T=0, the obtained H-T phase diagram suggests that the QCP is always accompanied by the breakdown of the SC order

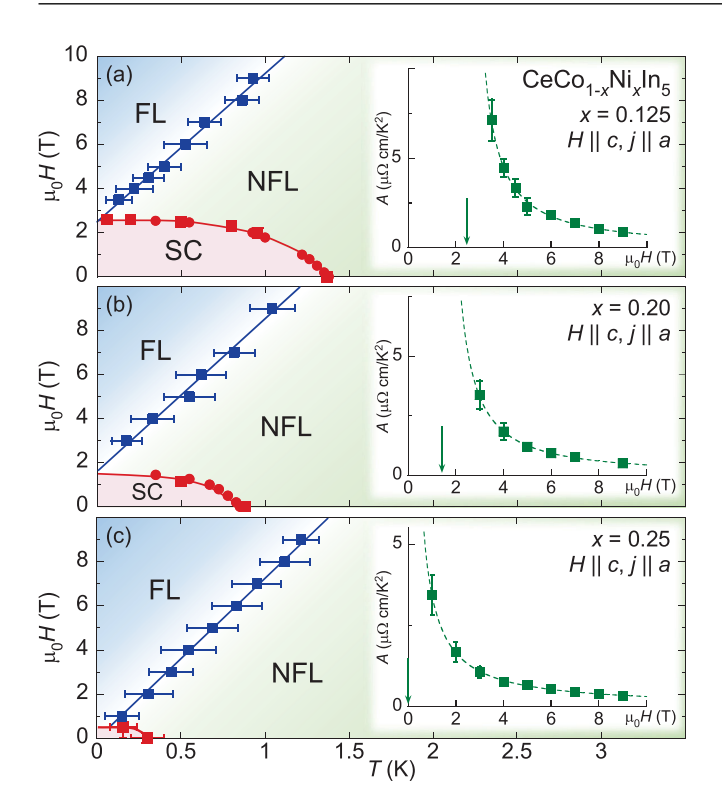


FIG. 2. Magnetic field versus temperature phase diagram for $\operatorname{CeCo}_{1-x}\operatorname{Ni}_x\operatorname{In}_5$ with (a) x=0.125, (b) 0.2, and (c) 0.25, obtained by the present ρ data (square) and the previous ρ and magnetization data (circle) [49]. The error bars of H_{c2} and T_c for x=0.125 and 0.2 are smaller than the marker size. The estimation of the error bars of $T_{\rm FL}$ is described in the Supplemental Material [56]. The insets show the H variations of the A coefficient defined by the $\rho=\rho_0+AT^2$ relation in the FL region. The errors in A are obtained by fitting the $\rho(T)$ data along with taking account of the ambiguity caused by the errors in $T_{\rm FL}$. The dashed curves and the arrows in the insets indicate the fitting results of $A(H)=A_0\mu_0^\alpha(H-H^*)^\alpha$ and H^* , respectively.

at H_{c2} regardless of the suppression of the SC order by the Ni doping.

The location of the OCP can also be derived from the diverging behavior in the A coefficient of the T^2 term in $\rho(T)$, as shown in the insets in Figs. 2(a)-2(c). In accordance with the analyses executed for the $\rho(T)$ data of CeCoIn₅ [20], we assumed the phenomenological relation of $A(H) = A_0 \mu_0^{\alpha} (H - H)$ H^*) $^{\alpha}$ for the field variations of the A coefficient, estimated from the $\rho(T)$ data for $T < T_{FL}$ [Figs. 1(a)–1(c)]. The relation above well traces the A values for $x \leq 0.25$, and the best fit gives $\mu_0 H^*$ to be 2.4(1) T (x = 0.125), 1.5(1) T (x = 0.2), and 0.0(4) T (x = 0.25). These values are close to $H_{c2}(T = 0)$ [Figs. 2(a)–2(c)] and are consistent with the locations of the QCP derived from $T_{\rm FL}$. The features above concerning the SC phase and the quantum criticality, namely, the relation of $H^* \sim H_{c2}$ and the diverging behavior in A(H) toward H^* , are common in Ni- and Sn-doped CeCoIn₅ [46], supporting the argument that the electron-doping effect is dominant in the physics related to the SC and NFL states in those alloys. We summarized the SC phase boundary, the NFL and FL regions, and the locations of the QCP in the T-H-x phase diagram of Ni-doped CeCoIn₅ [Fig. 3(a)].

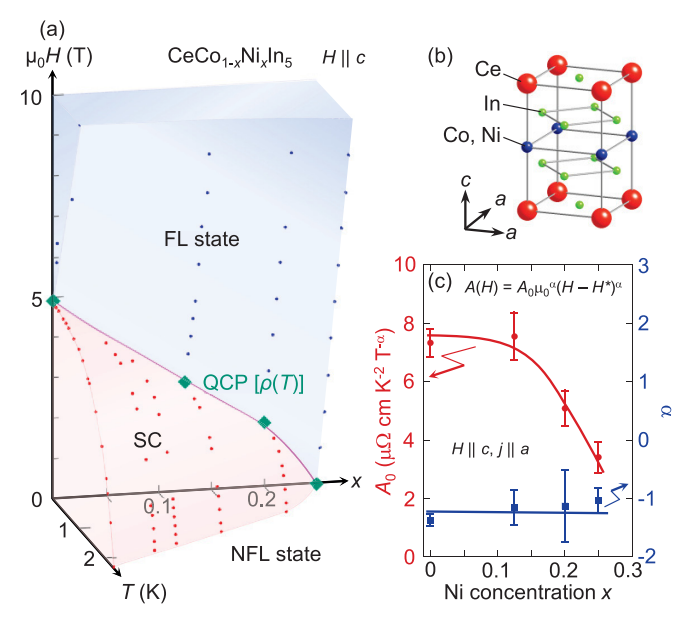


FIG. 3. (a) The T-H-x phase diagram for $CeCo_{1-x}Ni_xIn_5$, obtained from the $\rho(T)$ data and the previous magnetization, electrical resistivity, and specific heat experiments [8,20,49]. Diamond markers represent the locations of the QCP, corresponding to H^* . Panel (b) shows the crystal structure of $CeCo_{1-x}Ni_xIn_5$. (c) The Ni concentration dependence of the parameters A_0 (left axis) and that of α (right axis) in the fitting function of $A(H) = A_0\mu_0^{\alpha}(H - H^*)^{\alpha}$, plotted in the insets in Figs. 2(a)–2(c). The error bars in these parameters are estimated by the fitting analysis, along with taking account of the large ambiguity in A at $\sim H_{c2}$ (see the insets in Fig. 2). The data for pure $CeCoIn_5$ in panel (c) are obtained from Ref. [20].

The characteristics of the quantum criticality in Ni-doped $CeCoIn_5$ can further be argued from the parameters α and A_0 in $A(H) = A_0 \mu_0^{\alpha} (H - H^*)^{\alpha}$. Figure 3(c) shows the Ni concentration dependence of the parameters A_0 (left axis) and that of α (right axis). The exponent α is roughly independent of x with a value of about -1, while its QCP moves from finite to zero fields with x. Interestingly, the relation of $\alpha \sim -1$ is also realized in the typical quantum critical compound YbRh₂Si₂ [52]. The origin of the $\alpha \sim -1$ relation is unclear in Ni-doped CeCoIn₅. Theoretical calculations for the AFM quantum critical fluctuations may provide a clue for understanding this relation. A reduction of A_0 above $x \sim 0.2$ implies that the spin fluctuations are weakened with x because the magnitude A_0 is expected to reflect the strength of the spin fluctuations. This is consistent with the argument that Ni doping separates the system away from the region $(x \sim 0)$ involving the most enhanced AFM quantum critical fluctuations [51]. A similar trend is also found in the $-\ln T$ diverging behavior in specific heat; the coefficient of the $-\ln T$ function at the critical field for x = 0.25 is about a quarter of that for x = 0 [19,50]. In contrast to the features above concerning the quantum criticality, the residual resistivity $\rho(T \to 0)$ at H^* monotonously increases from 5.6 (x = 0.125) to 10 $\mu\Omega$ cm (x = 0.25) [Figs. 1(a)–1(c)], mainly reflecting the impurityscattering effect due to the Ni doping.

We briefly describe the feature in magnetoresistance for the Ni-doped alloys. In CeCoIn₅, a peak emerging in the field variations of the resistivity $\rho(H)$ provides an additional

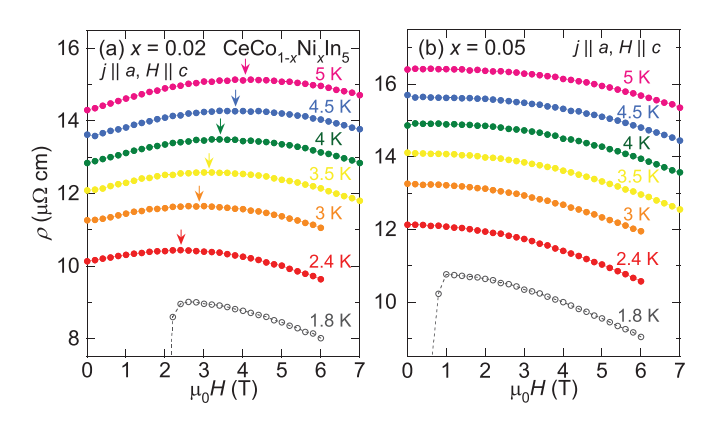


FIG. 4. Magnetic field variations of electrical resistivity for $CeCo_{1-x}Ni_xIn_5$ with (a) x = 0.02 and (b) x = 0.05. The arrows in panel (a) indicate the peak positions.

boundary dividing the H-T space into positive and negative $d\rho/dH$ regions, and an extrapolation of this boundary to zero temperature roughly coincides with the QCP ($\sim H_{c2}$) [20]. A similar feature is also confirmed in the Ni concentration of x=0.02 [Fig. 4(a)]. However, the $\rho(H)$ curve involves no peak and shows a monotonic decrease with H for x=0.05 [Fig. 4(b)] despite the QCP at $\sim H_{c2}$ being stable for x up to 0.25. This implies a weak or no coupling between this boundary and the QCP. It rather appears that spin fluctuations yielding $d\rho/dH < 0$ in the high-field range persist up to 25% Ni concentration, although those causing $d\rho/dH > 0$ in the low fields are quickly suppressed with the Ni doping. This trend seems consistent with the relation of $H_{c2} \sim H^*$ realized up to x=0.25, while H_{c2} decreases to zero.

The present resistivity study for $CeCo_{1-x}Ni_xIn_5$ revealed that the critical field H^* , regarded as the QCP, decreases to zero in connection with the suppression of H_{c2} with x. In addition, the continuous reduction of H^* with x suggests that the nature of the spin fluctuations causing the QCP has not changed significantly by the Ni doping for $x \le 0.25$. Meanwhile, doping Zn ions into CeCoIn $_5$ can induce the AFM orders, and the order parameter of the field-induced incommensurate AFM phase in the Zn-doped alloys is considered an origin of the quantum critical fluctuations at $\sim H_{c2}$ in CeCoIn $_5$ [36,37]. According to the doping effects above, the incommensurate AFM order parameter is expected to cause the quantum critical behavior in Ni-doped CeCoIn $_5$ entirely.

In general, quantum criticality originating from a hidden AFM order parameter should be enhanced at zero fields because the uniform magnetic field is unfavorable to the AFM spin correlations. In this context, it is natural to expect that the SC order pushes up the AFM QCP away from H=0 for x<0.25 because of a competition between the SC and incommensurate AFM orders, yielding nearly the same critical fields of H_{c2} and H^* , as revealed by the present investigations. This interpretation contrasts with that obtained by the $\rho(T)$ measurements under pressure for CeCoIn₅; H^* rapidly decreases with pressure and enters into the SC phase ($H^* < H_{c2}$) [57]. This discrepancy in H^* between the Ni-doped alloys

and the pure compound under pressure may occur because the different fluctuating AFM modes are traced in each $\rho(T)$ measurement. It was revealed that the QCP of the commensurate AFM order, instead of the incommensurate AFM order responsible for the QCP in the Ni-doped alloys, can exist within the SC phase in Zn-doped CeCoIn₅ [38]. The QCP of the other incommensurate AFM state related to the Q phase is also likely located within the SC phase in Nd-doped CeCoIn₅ [42]. Importantly, the scaling analysis on the magnetic Grüneisen ratio for CeCoIn₅ suggests that the QCP is located at zero magnetic fields rather than $\sim H_{c2}$ [18]. In this regard, it is interesting to measure the magnetic Grüneisen ratio of the Ni-doped alloys to further clarify the nature of the QCP. If such a measurement reveals the emergence of the zero-field QCP in the entire Ni concentrations in contrast to the present findings in $\rho(T)$, it is considered that multiple AFM modes contribute to the quantum criticality in pure and Ni-doped CeCoIn₅, which appear in different forms between those quantities.

Thus far, the relationship between the quantum critical behavior at $\sim H_{c2}$ and the Fulde–Ferrell–Larkin–Ovchinnikov (FFLO) phase possibly detected just below H_{c2} [17,58–61] has not yet been clarified in CeCoIn₅. The Ni-doped alloys would be a good platform to investigate this relationship because the strong Pauli-limited condition on H_{c2} is unchanged there [49]. However, it is also unclear whether the FFLO phase survives in connection with the reduction of H_{c2} in Ni-doped CeCoIn₅. We thus plan to perform ultrasonic sound velocity and nuclear magnetic resonance measurements for Ni-doped CeCoIn₅ [60,62]. Similar investigations may provide further information on the relationship between the quantum critical fluctuations and the possible field-induced AFM ordering at extremely low temperatures ($T \sim 20 \text{ mK}$) in CeCoIn₅ [44,45]. In addition, it is interesting to investigate the anisotropy in the emergence of the field-induced QCP in Ni-doped CeCoIn₅, because the QCP likely exists at $\sim H_{c2}$ (11.8 T) for $H \perp c$ in CeCoIn₅, similar to the situation for $H \parallel c$ [63]. The investigations above would provide a key to understanding the origin of the quantum critical behavior and its relationship with the SC order.

In conclusion, our $\rho(T)$ measurements for $\text{CeCo}_{1-x}\text{Ni}_x\text{In}_5$ $(x\leqslant 0.25)$ revealed the emergence of the NFL and FL states under H. The NFL-FL boundary for $T\to 0$, at which the QCP is expected to be located, roughly coincides with $H_{c2}(T=0)$ for the entire x range investigated. Furthermore, the A coefficient of the T^2 term in $\rho(T)$, estimated in the FL region, shows the diverging behavior with decreasing H toward H_{c2} . These experimental results suggest that the emergence of the QCP is always connected with the breakdown of the SC state at H_{c2} , and this is caused by the identical hidden AFM order parameter among the Ni concentrations.

M.Y. expresses gratitude to H. Sakai for helpful discussions. A part of this research was carried out as joint research at the Institute for Materials Research, Tohoku University, and was supported by Japan Society for the Promotion of Science KAKENHI Grants No. 17K05529, No. 20K03852, No. 23K03315, and No. 23H01128.

- [1] G. R. Stewart, Rev. Mod. Phys. 83, 1589 (2011).
- [2] N. D. Mathur, F. M. Grosche, S. R. Julian, I. R. Walker, D. M. Freye, R. K. W. Haselwimmer, and G. G. Lonzarich, Nature (London) 394, 39 (1998).
- [3] C. Pfleiderer, Rev. Mod. Phys. 81, 1551 (2009).
- [4] C. Petrovic, P. G. Pagliuso, M. F. Hundley, R. Movshovich, J. L. Sarrao, J. D. Thompson, Z. Fisk, and P. Monthoux, J. Phys.: Condens. Matter 13, L337 (2001).
- [5] K. Izawa, H. Yamaguchi, Y. Matsuda, H. Shishido, R. Settai, and Y. Onuki, Phys. Rev. Lett. 87, 057002 (2001).
- [6] W. K. Park, J. L. Sarrao, J. D. Thompson, and L. H. Greene, Phys. Rev. Lett. 100, 177001 (2008).
- [7] K. An, T. Sakakibara, R. Settai, Y. Onuki, M. Hiragi, M. Ichioka, and K. Machida, Phys. Rev. Lett. 104, 037002 (2010).
- [8] T. Tayama, A. Harita, T. Sakakibara, Y. Haga, H. Shishido, R. Settai, and Y. Onuki, Phys. Rev. B 65, 180504(R) (2002).
- [9] A. Bianchi, R. Movshovich, C. Capan, P. G. Pagliuso, and J. L. Sarrao, Phys. Rev. Lett. 91, 187004 (2003).
- [10] K. Kakuyanagi, M. Saitoh, K. Kumagai, S. Takashima, M. Nohara, H. Takagi, and Y. Matsuda, Phys. Rev. Lett. 94, 047602 (2005).
- [11] B.-L. Young, R. R. Urbano, N. J. Curro, J. D. Thompson, J. L. Sarrao, A. B. Vorontsov, and M. J. Graf, Phys. Rev. Lett. 98, 036402 (2007).
- [12] M. Kenzelmann, Th. Strassle, C. Niedermayer, M. Sigrist, B. Padmanabhan, M. Zolliker, A. D. Bianchi, R. Movshovich, E. D. Bauer, J. L. Sarrao, and J. D. Thompson, Science 321, 1652 (2008).
- [13] A. Aperis, G. Varelogiannis, P. B. Littlewood, and B. D. Simons, J. Phys.: Condens. Matter 20, 434235 (2008).
- [14] D. F. Agterberg, M. Sigrist, and H. Tsunetsugu, Phys. Rev. Lett. 102, 207004 (2009).
- [15] Y. Yanase, J. Phys. Soc. Jpn. 77, 063705 (2008).
- [16] Y. Yanase and M. Sigrist, J. Phys. Soc. Jpn. 78, 114715 (2009).
- [17] S. Kittaka, Y. Kono, K. Tsunashima, D. Kimoto, M. Yokoyama, Y. Shimizu, T. Sakakibara, M. Yamashita, and K. Machida, Phys. Rev. B 107, L220505 (2023).
- [18] Y. Tokiwa, E. D. Bauer, and P. Gegenwart, Phys. Rev. Lett. 111, 107003 (2013).
- [19] A. Bianchi, R. Movshovich, I. Vekhter, and P. G. Pagliuso, and J. L. Sarrao, Phys. Rev. Lett. **91**, 257001 (2003).
- [20] J. Paglione, M. A. Tanatar, D. G. Hawthorn, E. Boaknin, R. W. Hill, F. Ronning, M. Sutherland, L. Taillefer, C. Petrovic, and P. C. Canfield, Phys. Rev. Lett. 91, 246405 (2003).
- [21] L. Howald, G. Seyfarth, G. Knebel, G. Lapertot, D. Aoki, and J.-P. Brison, J. Phys. Soc. Jpn. **80**, 024710 (2011).
- [22] H. Sakai, S. E. Brown, S.-H. Baek, F. Ronning, E. D. Bauer, and J. D. Thompson, Phys. Rev. Lett. 107, 137001 (2011).
- [23] V. S. Zapf, E. J. Freeman, E. D. Bauer, J. Petricka, C. Sirvent, N. A. Frederick, R. P. Dickey, and M. B. Maple, Phys. Rev. B 65, 014506 (2001).
- [24] M. Yokoyama, H. Amitsuka, K. Matsuda, A. Gawase, N. Oyama, I. Kawasaki, K. Tenya, and H. Yoshizawa, J. Phys. Soc. Jpn. 75, 103703 (2006).
- [25] S. Ohira-Kawamura, H. Shishido, A. Yoshida, R. Okazaki, H. Kawano-Furukawa, T. Shibauchi, H. Harima, and Y. Matsuda, Phys. Rev. B 76, 132507 (2007).
- [26] M. Yokoyama, N. Oyama, H. Amitsuka, S. Oinuma, I. Kawasaki, K. Tenya, M. Matsuura, K. Hirota, and T. J. Sato, Phys. Rev. B 77, 224501 (2008).

- [27] S. K. Goh, J. Paglione, M. Sutherland, E. C. T. O'Farrell, C. Bergemann, T. A. Sayles, and M. B. Maple, Phys. Rev. Lett. 101, 056402 (2008).
- [28] L. D. Pham, T. Park, S. Maquilon, J. D. Thompson, and Z. Fisk, Phys. Rev. Lett. 97, 056404 (2006).
- [29] M. Nicklas, O. Stockert, T. Park, K. Habicht, K. Kiefer, L. D. Pham, J. D. Thompson, Z. Fisk, and F. Steglich, Phys. Rev. B 76, 052401 (2007).
- [30] R. R. Urbano, B.-L. Young, N. J. Curro, J. D. Thompson, L. D. Pham, and Z. Fisk, Phys. Rev. Lett. 99, 146402 (2007).
- [31] S. Seo, X. Lu, J.-X. Zhu, R. R. Urbano, N. Curro, E. D. Bauer, V. A. Sidorov, L. D. Pham, Tuson Park, Z. Fisk, and J. D. Thompson, Nat. Phys. 10, 120 (2014).
- [32] C. Stock, J. A. Rodriguez-Rivera, K. Schmalzl, F. Demmel, D. K. Singh, F. Ronning, J. D. Thompson, and E. D. Bauer, Phys. Rev. Lett. 121, 037003 (2018).
- [33] M. Yokoyama, K. Fujimura, S. Ishikawa, M. Kimura, T. Hasegawa, I. Kawasaki, K. Tenya, Y. Kono, and T. Sakakibara, J. Phys. Soc. Jpn. 83, 033706 (2014).
- [34] M. Yokoyama, H. Mashiko, R. Otaka, Y. Sakon, K. Fujimura, K. Tenya, A. Kondo, K. Kindo, Y. Ikeda, H. Yoshizawa, Y. Shimizu, Y. Kono, and T. Sakakibara, Phys. Rev. B 92, 184509 (2015).
- [35] M. Yokoyama, H. Mashiko, R. Otaka, Y. Oshima, K. Suzuki, K. Tenya, Y. Shimizu, A. Nakamura, D. Aoki, A. Kondo, K. Kindo, S. Nakamura, and T. Sakakibara, Phys. Rev. B 95, 224425 (2017).
- [36] H. Sakai, Y. Tokunaga, S. Kambe, J.-X. Zhu, F. Ronning, J. D. Thompson, S. K. Ramakrishna, A. P. Reyes, K. Suzuki, Y. Oshima, and M. Yokoyama, Phys. Rev. B 104, 085106 (2021).
- [37] M. Yokoyama, Y. Honma, Y. Oshima, Rahmanto, K. Suzuki, K. Tenya, Y. Shimizu, D. Aoki, A. Matsuo, K. Kindo, S. Nakamura, Y. Kono, S. Kittaka, and T. Sakakibara, Phys. Rev. B 105, 054515 (2022).
- [38] W. Higemoto, M. Yokoyama, T. U. Ito, T. Suzuki, S. Raymond, and Y. Yanase, Proc. Natl. Acad. Sci. 119, e2209549119 (2022).
- [39] M. Haze, Y. Torii, R. Peters, S. Kasahara, Y. Kasahara, T. Shibauchi, T. Terashima, and Y. Matsuda, J. Phys. Soc. Jpn. 87, 034702 (2018).
- [40] R. Hu, Y. Lee, J. Hudis, V. F. Mitrovic, and C. Petrovic, Phys. Rev. B 77, 165129 (2008).
- [41] S. Raymond, S. M. Ramos, D. Aoki, G. Knebel, V. P. Mineev, and G. Lapertot, J. Phys. Soc. Jpn. 83, 013707 (2014).
- [42] D. G. Mazzone, S. Raymond, J. L. Gavilano, E. Ressouche, C. Niedermayer, J. O. Birk, B. Ouladdiaf, G. Bastien, G. Knebel, D. Aoki, G. Lapertot, and M. Kenzelmann, Sci. Adv. 3, e1602055 (2017).
- [43] D. L. Kunwar, R. B. Adhikari, N. Pouse, M. B. Maple, M. Dzero, and C. C. Almasan, Phys. Rev. B 103, 224519 (2021).
- [44] H. Shishido, S. Yamada, K. Sugii, M. Shimozawa, Y. Yanase, and M. Yamashita, Phys. Rev. Lett. **120**, 177201 (2018).
- [45] M. Yamashita, M. Tashiro, K. Saiki, S. Yamada, M. Akazawa, M. Shimozawa, T. Taniguchi, H. Takeda, M. Takigawa, and H. Shishido, Phys. Rev. B 102, 165154 (2020).
- [46] E. D. Bauer, C. Capan, F. Ronning, R. Movshovich, J. D. Thompson, and J. L. Sarrao, Phys. Rev. Lett. 94, 047001 (2005).
- [47] E. D. Bauer, F. Ronning, C. Capan, M. J. Graf, D. Vandervelde, H. Q. Yuan, M. B. Salamon, D. J. Mixson, N. O. Moreno, S. R. Brown, J. D. Thompson, R. Movshovich, M. F. Hundley, J. L.

- Sarrao, P. G. Pagliuso, and S. M. Kauzlarich, Phys. Rev. B 73, 245109 (2006).
- [48] S. M. Ramos, M. B. Fontes, E. N. Hering, M. A. Continentino, E. Baggio-Saitovich, F. D. Neto, E. M. Bittar, P. G. Pagliuso, E. D. Bauer, J. L. Sarrao, and J. D. Thompson, Phys. Rev. Lett. 105, 126401 (2010).
- [49] R. Otaka, M. Yokoyama, H. Mashiko, T. Hasegawa, Y. Shimizu, Y. Ikeda, K. Tenya, S. Nakamura, D. Ueta, H. Yoshizawa, and T. Sakakibara, J. Phys. Soc. Jpn. 85, 094713 (2016).
- [50] M. Yokoyama, K. Suzuki, K. Tenya, S. Nakamura, Y. Kono, S. Kittaka, and T. Sakakibara, Phys. Rev. B 99, 054506 (2019).
- [51] H. Sakai, Y. Tokunaga, S. Kambe, J.-X. Zhu, F. Ronning, J. D. Thompson, H. Kotegawa, H. Tou, K. Suzuki, Y. Oshima, and M. Yokoyama, Phys. Rev. B 106, 235152 (2022).
- [52] P. Gegenwart, J. Custers, C. Geibel, K. Neumaier, T. Tayama, K. Tenya, O. Trovarelli, and F. Steglich, Phys. Rev. Lett. 89, 056402 (2002).
- [53] S. Araki, M. Nakashima, R. Settai, T. C. Kobayashi, and Y. Onuki, J. Phys.: Condens. Matter 14, L377 (2002).
- [54] M. Ohashi, F. Honda, T. Eto, S. Kaji, I. Minamitake, G. Oomi, S. Koiwai, and Y. Uwatoko, Physica B: Condens. Matter 312-313, 443 (2002).

- [55] G. Knebel, D. Aoki, J.-P. Brison, and J. Flouquet, J. Phys. Soc. Jpn. 77, 114704 (2008).
- [56] See Supplemental Material at http://link.aps.org/supplemental/ 10.1103/PhysRevMaterials.8.L081801 for details on the estimation of crossover temperature from the non-Fermi-liquid to Fermi-liquid states.
- [57] F. Ronning, C. Capan, E. D. Bauer, J. D. Thompson, J. L. Sarrao, and R. Movshovich, Phys. Rev. B 73, 064519 (2006).
- [58] P. Fulde and R. A. Ferrell, Phys. Rev. 135, A550 (1964).
- [59] A. I. Larkin and Y. N. Ovchinnikov, Zh. Eksp. Teor. Fiz. 47, 1136 (1964).
- [60] K. Kumagai, M. Saitoh, T. Oyaizu, Y. Furukawa, S. Takashima, M. Nohara, H. Takagi, and Y. Matsuda, Phys. Rev. Lett. 97, 227002 (2006).
- [61] S.-Z. Lin, D. Y. Kim, E. D. Bauer, F. Ronning, J. D. Thompson, and R. Movshovich, Phys. Rev. Lett. 124, 217001 (2020).
- [62] T. Watanabe, Y. Kasahara, K. Izawa, T. Sakakibara, Y. Matsuda, C. J. van der Beek, T. Hanaguri, H. Shishido, R. Settai, and Y. Onuki, Phys. Rev. B 70, 020506(R) (2004).
- [63] F. Ronning, C. Capan, A. Bianchi, R. Movshovich, A. Lacerda, M. F. Hundley, J. D. Thompson, P. G. Pagliuso, and J. L. Sarrao, Phys. Rev. B 71, 104528 (2005).